

The Flow of Newtonian Fluids in Axisymmetric Corrugated Tubes

Taha Sochi*

June 9, 2010

*University College London, Department of Physics & Astronomy, Gower Street, London, WC1E 6BT. Email: t.sochi@ucl.ac.uk.

Contents

Contents	2
List of Figures	3
Abstract	4
1 Introduction	5
2 Correlation Between Pressure Drop and Flow Rate	6
2.1 Conical Tube	7
2.2 Parabolic Tube	8
2.3 Hyperbolic Tube	10
2.4 Hyperbolic Cosine Tube	11
2.5 Sinusoidal Tube	11
3 Conclusions	14
Nomenclature	14
References	15

List of Figures

1	Profiles of converging-diverging axisymmetric capillaries.	6
2	Schematic representation of the radius of a conically shaped converging-diverging capillary as a function of the distance along the tube axis.	8
3	Schematic representation of the radius of a converging-diverging capillary with a parabolic profile as a function of the distance along the tube axis.	9
4	Schematic representation of the radius of a converging-diverging capillary with a sinusoidal profile as a function of the distance along the tube axis.	12

Abstract

This article deals with the flow of Newtonian fluids through axially-symmetric corrugated tubes. An analytical method to derive the relation between volumetric flow rate and pressure drop in laminar flow regimes is presented and applied to a number of simple tube geometries of converging-diverging nature. The method is general in terms of fluid and tube shape within the previous restrictions. Moreover, it can be used as a basis for numerical integration where analytical relations cannot be obtained due to mathematical difficulties.

1 Introduction

Modeling the flow through corrugated tubes of various geometries is an important subject and has many real-life applications. Moreover, it is required for modeling viscoelasticity, yield-stress and the flow of Newtonian and non-Newtonian fluids through porous media [1–3]. There are many previous attempts to model the flow through capillaries of different geometries. However, they either apply to tubes of regular cross sections [4, 5] or deal with very special cases. Most of these studies use numerical mesh techniques such as finite difference and spectral methods to obtain numerical results. Illuminating examples of these investigations are Kozicki *et al.* [6], Miller [7], Oka [8], Williams and Javadpour [9], Phan-Thien *et al.* [10, 11], Lahbabi and Chang [12], Burdette *et al.* [13], Pilitsis *et al.* [14, 15], James *et al.* [16], Talwar and Khomami [17], Koshiba *et al.* [18], Masuleh and Phillips [19], and Davidson *et al.* [20].

In the current paper we present an analytical method for deriving the relationship between pressure drop and volumetric flow rate in corrugated tubes of circular but varying cross section, such as those depicted schematically in Figure 1. We also present several examples of the use of this method to derive equations for Newtonian flow although the method is general and can be applied to non-Newtonian flow as well. In the following derivations we assume a laminar flow of a purely-viscous incompressible fluid where the tube corrugation is smooth and limited in magnitude to avoid problematic flow phenomena such as vortices.

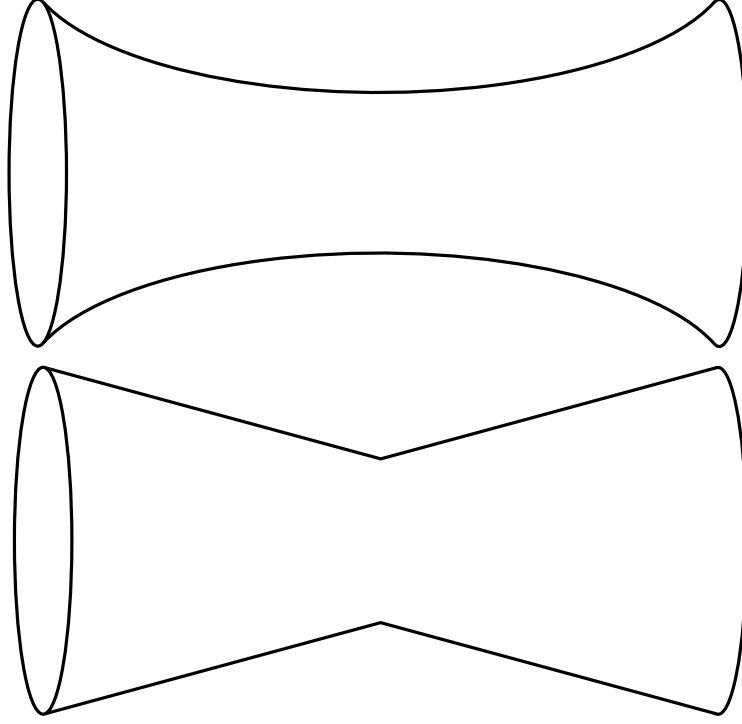


Figure 1: Profiles of converging-diverging axisymmetric capillaries.

2 Correlation Between Pressure Drop and Flow Rate

A Newtonian fluid with a viscosity μ satisfy the following relation between stress τ and strain rate $\dot{\gamma}$

$$\tau = \mu\dot{\gamma} \quad (1)$$

The Hagen-Poiseuille equation for a Newtonian fluid passing through a cylindrical pipe of constant circular cross section, which can be derived directly from Equation 1, states that

$$Q = \frac{\pi r^4 P}{8\mu x} \quad (2)$$

where Q is the volumetric flow rate, r is the tube radius, P is the pressure drop across the tube, μ is the fluid viscosity and x is the tube length. A derivation of this relation can be found, for example, in [1, 21]. On solving this equation for P ,

the following expression for pressure drop as a function of flow rate is obtained

$$P = \frac{8Q\mu x}{\pi r^4} \quad (3)$$

For an infinitesimal length, δx , of a capillary, the infinitesimal pressure drop for a given flow rate Q is given by

$$\delta P = \frac{8Q\mu\delta x}{\pi r^4} \quad (4)$$

For an incompressible fluid, the volumetric flow rate across an arbitrary cross section of the capillary is constant. Therefore, the total pressure drop across a capillary of length L with circular cross section of varying radius, $r(x)$, is given by

$$P = \frac{8Q\mu}{\pi} \int_0^L \frac{dx}{r^4} \quad (5)$$

This relation will be used in the following sections to derive relations between pressure drop and volumetric flow rate for a number of geometries of axisymmetric capillaries of varying cross section with converging-diverging feature. The method can be equally applied to other geometries of different nature.

2.1 Conical Tube

For a corrugated tube of conical shape, depicted in Figure 2, the radius r as a function of the axial coordinate x in the designated frame is given by

$$r(x) = a + b|x| \quad -L/2 \leq x \leq L/2 \quad (6)$$

where

$$a = R_{min} \quad \text{and} \quad b = \frac{2(R_{max} - R_{min})}{L} \quad (7)$$

Hence, Equation 5 becomes

$$P = \frac{8Q\mu}{\pi} \int_{-L/2}^{L/2} \frac{dx}{(a + b|x|)^4} \quad (8)$$

$$= \frac{8Q\mu}{\pi} \left[\frac{1}{3b(a - bx)^3} \right]_{-L/2}^0 + \frac{8Q\mu}{\pi} \left[-\frac{1}{3b(a + bx)^3} \right]_0^{L/2} \quad (9)$$

$$= \frac{16Q\mu}{\pi} \left[\frac{1}{3a^3b} - \frac{1}{3b(a + bL/2)^3} \right] \quad (10)$$

that is

$$P = \frac{8LQ\mu}{3\pi(R_{max} - R_{min})} \left[\frac{1}{R_{min}^3} - \frac{1}{R_{max}^3} \right] \quad (11)$$

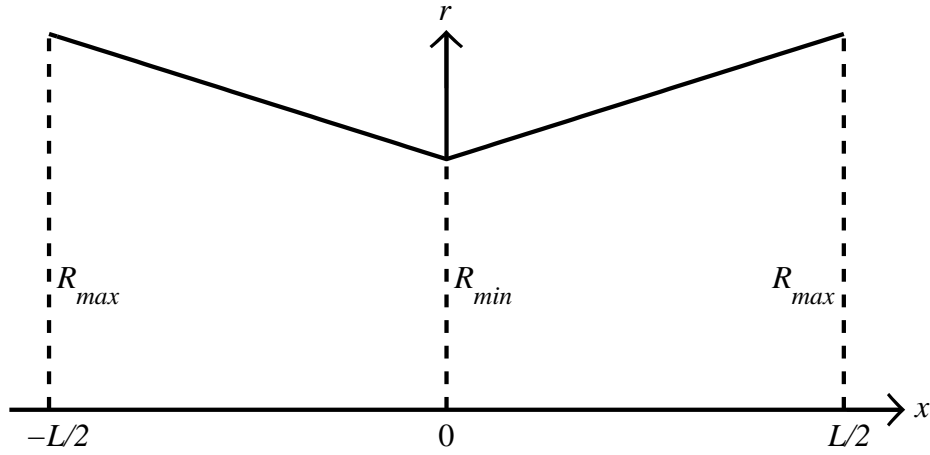


Figure 2: Schematic representation of the radius of a conically shaped converging-diverging capillary as a function of the distance along the tube axis.

2.2 Parabolic Tube

For a tube of parabolic profile, depicted in Figure 3, the radius is given by

$$r(x) = a + bx^2 \quad -L/2 \leq x \leq L/2 \quad (12)$$

where

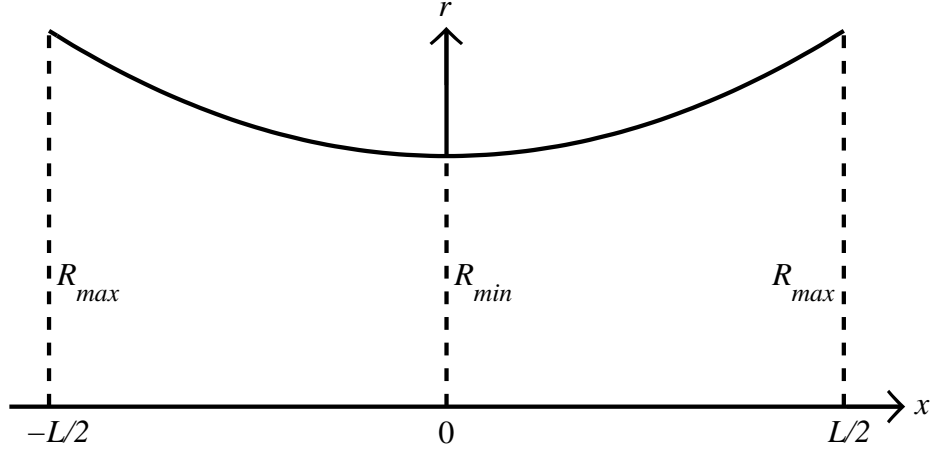


Figure 3: Schematic representation of the radius of a converging-diverging capillary with a parabolic profile as a function of the distance along the tube axis.

$$a = R_{min} \quad \text{and} \quad b = \left(\frac{2}{L}\right)^2 (R_{max} - R_{min}) \quad (13)$$

Therefore, Equation 5 becomes

$$P = \frac{8Q\mu}{\pi} \int_{-L/2}^{L/2} \frac{dx}{(a + bx^2)^4} \quad (14)$$

On performing this integration, the following relation is obtained

$$P = \frac{8Q\mu}{\pi} \left[\frac{x}{6a(a + bx^2)^3} + \frac{5x}{24a^2(a + bx^2)^2} + \frac{5x}{16a^3(a + bx^2)} + \frac{5 \arctan\left(x\sqrt{\frac{b}{a}}\right)}{16a^{7/2}\sqrt{b}} \right]_{-L/2}^{L/2} \quad (15)$$

$$= \frac{8Q\mu}{\pi} \left[\frac{L}{6a[a + b(L/2)^2]^3} + \frac{5L}{24a^2[a + b(L/2)^2]^2} + \frac{5L}{16a^3[a + b(L/2)^2]} + \frac{10 \arctan\left(\frac{L}{2}\sqrt{\frac{b}{a}}\right)}{16a^{7/2}\sqrt{b}} \right] \quad (16)$$

that is

$$P = \frac{4LQ\mu}{\pi} \left[\frac{1}{3R_{min}R_{max}^3} + \frac{5}{12R_{min}^2R_{max}^2} + \frac{5}{8R_{min}^3R_{max}} + \frac{5 \arctan \left(\sqrt{\frac{R_{max}-R_{min}}{R_{min}}} \right)}{8R_{min}^{7/2} \sqrt{R_{max}-R_{min}}} \right] \quad (17)$$

2.3 Hyperbolic Tube

For a tube of hyperbolic profile, similar to the profile in Figure 3, the radius is given by

$$r(x) = \sqrt{a + bx^2} \quad -L/2 \leq x \leq L/2 \quad a, b > 0 \quad (18)$$

where

$$a = R_{min}^2 \quad \text{and} \quad b = \left(\frac{2}{L} \right)^2 (R_{max}^2 - R_{min}^2) \quad (19)$$

Therefore, Equation 5 becomes

$$P = \frac{8Q\mu}{\pi} \int_{-L/2}^{L/2} \frac{dx}{(a + bx^2)^2} \quad (20)$$

$$= \frac{8Q\mu}{\pi} \left[\frac{x}{2a(a + bx^2)} + \frac{\arctan(x\sqrt{b/a})}{2a\sqrt{ab}} \right]_{-L/2}^{L/2} \quad (21)$$

that is

$$P = \frac{4LQ\mu}{\pi} \left[\frac{1}{R_{min}^2 R_{max}^2} + \frac{\arctan \left(\sqrt{\frac{R_{max}^2 - R_{min}^2}{R_{min}^2}} \right)}{R_{min}^3 \sqrt{R_{max}^2 - R_{min}^2}} \right] \quad (22)$$

2.4 Hyperbolic Cosine Tube

For a tube of hyperbolic cosine profile, similar to the profile in Figure 3, the radius is given by

$$r(x) = a \cosh(bx) \quad -L/2 \leq x \leq L/2 \quad (23)$$

where

$$a = R_{min} \quad \text{and} \quad b = \frac{2}{L} \operatorname{arccosh} \left(\frac{R_{max}}{R_{min}} \right) \quad (24)$$

Hence, Equation 5 becomes

$$P = \frac{8Q\mu}{\pi} \int_{-L/2}^{L/2} \frac{dx}{[a \cosh(bx)]^4} \quad (25)$$

$$= \frac{8Q\mu}{\pi} \left[\frac{\tanh(bx) [\operatorname{sech}^2(bx) + 2]}{3a^4b} \right]_{-L/2}^{L/2} \quad (26)$$

that is

$$P = \frac{8LQ\mu}{3\pi R_{min}^4} \left[\frac{\tanh \left(\operatorname{arccosh} \left(\frac{R_{max}}{R_{min}} \right) \right) \left[\operatorname{sech}^2 \left(\operatorname{arccosh} \left(\frac{R_{max}}{R_{min}} \right) \right) + 2 \right]}{\operatorname{arccosh} \left(\frac{R_{max}}{R_{min}} \right)} \right] \quad (27)$$

2.5 Sinusoidal Tube

For a tube of sinusoidal profile, depicted in Figure 4, where the tube length L spans one complete wavelength, the radius is given by

$$r(x) = a - b \cos(kx) \quad -L/2 \leq x \leq L/2 \quad a > b > 0 \quad (28)$$

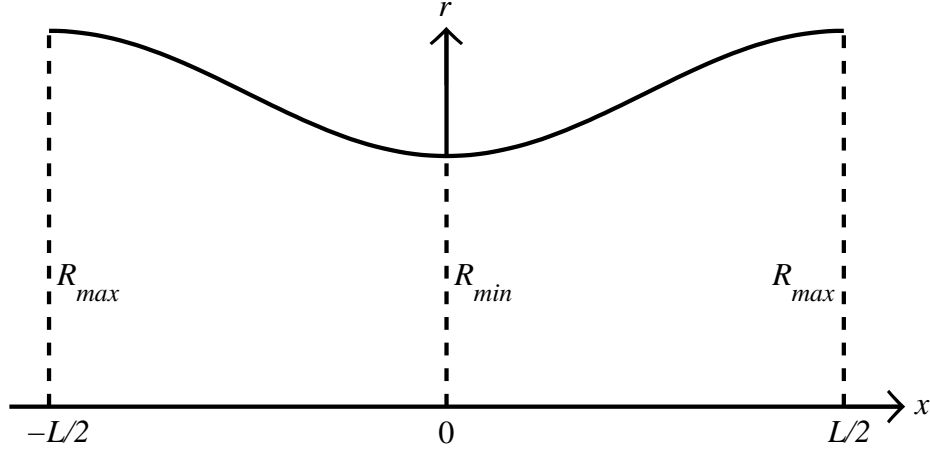


Figure 4: Schematic representation of the radius of a converging-diverging capillary with a sinusoidal profile as a function of the distance along the tube axis.

where

$$a = \frac{R_{max} + R_{min}}{2} \quad b = \frac{R_{max} - R_{min}}{2} \quad \& \quad k = \frac{2\pi}{L} \quad (29)$$

Hence, Equation 5 becomes

$$P = \frac{8Q\mu}{\pi} \int_{-L/2}^{L/2} \frac{dx}{[a - b \cos(kx)]^4} \quad (30)$$

On performing this integration, the following relation is obtained

$$P = \frac{8Q\mu}{\pi b^4 k} [I]_{-L/2}^{L/2} \quad (31)$$

where

$$I = \frac{(6A^3 + 9A)}{3(A^2 - 1)^{7/2}} \arctan \left(\frac{(A - 1) \tan(\frac{kx}{2})}{\sqrt{A^2 - 1}} \right) - \frac{(11A^2 + 4) \sin(kx)}{6(A^2 - 1)^3 [A + \cos(kx)]} \\ - \frac{5A \sin(kx)}{6(A^2 - 1)^2 [A + \cos(kx)]^2} - \frac{\sin(kx)}{3(A^2 - 1) [A + \cos(kx)]^3} \quad (32)$$

$$\& \quad A = \frac{R_{max} + R_{min}}{R_{min} - R_{max}} \quad (33)$$

On taking $\lim_{x \rightarrow -\frac{L}{2}^+} I$ and $\lim_{x \rightarrow \frac{L}{2}^-} I$ the following expression is obtained

$$P = \frac{8Q\mu}{\pi b^4 k} \left[-\frac{(6A^3 + 9A)}{3(A^2 - 1)^{7/2}} \frac{\pi}{2} - \frac{(6A^3 + 9A)}{3(A^2 - 1)^{7/2}} \frac{\pi}{2} \right] \quad (34)$$

$$= -\frac{8Q\mu(6A^3 + 9A)}{3b^4 k(A^2 - 1)^{7/2}} \quad (35)$$

Since $A < -1$, $P > 0$ as it should be. On substituting for A , b and k in the last expression we obtain

$$P = \frac{LQ\mu(R_{max} - R_{min})^3 \left[2 \left(\frac{R_{max} + R_{min}}{R_{max} - R_{min}} \right)^3 + 3 \left(\frac{R_{max} + R_{min}}{R_{max} - R_{min}} \right) \right]}{2\pi(R_{max}R_{min})^{7/2}} \quad (36)$$

that is

$$P = \frac{LQ\mu [2(R_{max} + R_{min})^3 + 3(R_{max} + R_{min})(R_{max} - R_{min})^2]}{2\pi(R_{max}R_{min})^{7/2}} \quad (37)$$

It is noteworthy that all these relations (i.e. Equations 11, 17, 22, 27 and 37), are dimensionally consistent. Moreover, they have been extensively tested and verified by numerical integration.

3 Conclusions

The current paper proposes an analytical method for deriving mathematical relations between pressure drop and volumetric flow rate in axially symmetric corrugated tubes of varying cross section. This method is applied on a number of converging-diverging capillary geometries in the context of Newtonian flow. The method can be equally applied to some cases of non-Newtonian flow within the given restrictions. It can also be extended to include other regular but non-axially-symmetric geometries. The method can be used as a basis for numerical integration when analytical solutions are out of reach due to mathematical complexities.

Nomenclature

$\dot{\gamma}$	strain rate (s^{-1})
μ	fluid viscosity (Pa.s)
τ	stress (Pa)
L	tube length (m)
P	pressure drop (Pa)
Q	volumetric flow rate ($\text{m}^3.\text{s}^{-1}$)
r	tube radius (m)
R_{max}	maximum radius of corrugated tube (m)
R_{min}	minimum radius of corrugated tube (m)
x	axial coordinate (m)

References

- [1] T. Sochi; M.J. Blunt. Pore-scale network modeling of Ellis and Herschel-Bulkley fluids. *Journal of Petroleum Science and Engineering*, 60(2):105–124, 2008. [5](#), [6](#)
- [2] T. Sochi. Pore-scale modeling of viscoelastic flow in porous media using a Bautista-Manero fluid. *International Journal of Heat and Fluid Flow*, 30(6):1202–1217, 2009. [5](#)
- [3] T. Sochi. Modelling the flow of yield-stress fluids in porous media. *Transport in Porous Media*, 2010. DOI: 10.1007/s11242-010-9574-z. [5](#)
- [4] F.M. White. *Viscous Fluid Flow*. McGraw Hill Inc., second edition, 1991. [5](#)
- [5] S. Sisavath; X. Jing; R.W. Zimmerman. Laminar flow through irregularly-shaped pores in sedimentary rocks. *Transport in Porous Media*, 45(1):41–62, 2001. [5](#)
- [6] W. Kozicki; C.H. Chou; C. Tiu. Non-Newtonian flow in ducts of arbitrary cross-sectional shape. *Chemical Engineering Science*, 21(8):665–679, 1966. [5](#)
- [7] C. Miller. Predicting non-Newtonian flow behavior in ducts of unusual cross section. *Industrial & Engineering Chemistry Fundamentals*, 11(4):524–528, 1972. [5](#)
- [8] S. Oka. Pressure development in a non-Newtonian flow through a tapered tube. *Rheologica Acta*, 12(2):224–227, 1973. [5](#)
- [9] E.W. Williams; S.H. Javadpour. The flow of an elastico-viscous liquid in an axisymmetric pipe of slowly varying cross-section. *Journal of Non-Newtonian Fluid Mechanics*, 7(2-3):171–188, 1980. [5](#)

- [10] N. Phan-Thien; C.J. Goh; M.B. Bush. Viscous flow through corrugated tube by boundary element method. *Journal of Applied Mathematics and Physics (ZAMP)*, 36(3):475–480, 1985. [5](#)
- [11] N. Phan-Thien; M.M.K. Khan. Flow of an Oldroyd-type fluid through a sinusoidally corrugated tube. *Journal of Non-Newtonian Fluid Mechanics*, 24:203–220, 1987. [5](#)
- [12] A. Lahbabi; H-C Chang. Flow in periodically constricted tubes: Transition to inertial and nonsteady flows. *Chemical Engineering Science*, 41(10):2487–2505, 1986. [5](#)
- [13] S.R. Burdette; P.J. Coates; R.C. Armstrong; R.A. Brown. Calculations of viscoelastic flow through an axisymmetric corrugated tube using the explicitly elliptic momentum equation formulation (EEME). *Journal of Non-Newtonian Fluid Mechanics*, 33(1):1–23, 1989. [5](#)
- [14] S. Pilitsis; A. Souvaliotis; A.N. Beris. Viscoelastic flow in a periodically constricted tube: The combined effect of inertia, shear thinning, and elasticity. *Journal of Rheology*, 35(4):605–646, 1991. [5](#)
- [15] S. Pilitsis; A.N. Beris. Calculations of steady-state viscoelastic flow in an undulating tube. *Journal of Non-Newtonian Fluid Mechanics*, 31(3):231–287, 1989. [5](#)
- [16] D.F. James; N. Phan-Thien; M.M.K. Khan; A.N. Beris; S. Pilitsis. Flow of test fluid M1 in corrugated tubes. *Journal of Non-Newtonian Fluid Mechanics*, 35(2-3):405–412, 1990. [5](#)
- [17] K.K. Talwar; B. Khomami. Application of higher order finite element methods to viscoelastic flow in porous media. *Journal of Rheology*, 36(7):1377–1416, 1992. [5](#)

- [18] T. Koshiha; N. Mori; K. Nakamura; S. Sugiyama. Measurement of pressure loss and observation of the flow field in viscoelastic flow through an undulating channel. *Journal of Rheology*, 44(1):65–78, 2000. [5](#)
- [19] S.H. Momeni-Masuleh; T.N. Phillips. Viscoelastic flow in an undulating tube using spectral methods. *Computers & fluids*, 33(8):1075–1095, 2004. [5](#)
- [20] D. Davidson; G.L. Lehmann; E.J. Cottis. Horizontal capillary flow of a Newtonian liquid in a narrow gap between a plane wall and a sinusoidal wall. *Fluid Dynamics Research*, 40(11-12):779–802, 2008. [5](#)
- [21] T. Sochi. *Pore-Scale Modeling of Non-Newtonian Flow in Porous Media*. PhD thesis, Imperial College London, 2007. [6](#)